Technical Report

TR-06-38

Sensitivity of total stress to changes in externally applied water pressure in KBS-3 buffer bentonite

J F Harrington, D J Birchall

British Geological Survey
Chemical & Biological Hazards Programme
Kingsley Dunham Centre

April 2007

SKB

Sensitivity of total stress to changes in externally applied water pressure in KBS-3 buffer bentonite

J F Harrington, D J Birchall

British Geological Survey
Chemical & Biological Hazards Programme
Kingsley Dunham Centre

April 2007

Abstract

This report describes two laboratory tests undertaken to examine the effect of increasing pore-water pressure and its relationship to total stress and swelling pressure in KBS-3 specification bentonite. Laboratory data clearly demonstrate that at porewater pressures of 46 MPa the bentonite retains a significant component of its original swelling pressure. Analysis of the total stress data demonstrates significant hysteresis between ascending and descending porewater pressure histories. The amount of hysteresis appears to be linked to the magnitude of the porewater pressure applied to the specimen, suggesting some form of "stress memory" within the clay. By the end of the second test the average swelling pressure had increased from 7.2 MPa to 14.4 MPa, which if correct, has important implications for repository performance assessment. No evidence for classic liquefaction of the clay at high water pressures was observed in this experimental study.

Sammanfattning

Den här rapporten beskriver två laboratorieförsök som gjorts för att studera effekten av ett ökande porvattentryck och dess betydelse för totaltryck och svälltryck i en KBS-3 buffert bentonit. Experimentella data visar klart att även vid ett portryck på 46 MPa behåller bentoniten en signifikant andel av sitt ursprungliga svälltryck. En analys av data för totaltryck visar att det finns en avsevärd hysteres mellan stigande och sjunkande portryckssekvenser. Hysteresens omfattning verkar vara kopplad till magnituden av det porvattentryck som läggs på provet, vilket indikerar någon form av "tryckminne" hos bentoniten. Vid slutet av det andra testet hade svälltrycket i medeltal ökat från 7.2 MPa till 14.4 MPa, vilket om det är korrekt, kan ha betydelse för förvarets långsiktiga funktion. Inga som helst indikationer av klassiskt flyttillstånd i leran vid höga portryck kunde dock observeras i den här studien.

Executive summary

In the current Swedish repository design concept, composite copper and steel canisters containing spent nuclear fuel will be placed in large diameter disposal boreholes drilled into the floor of the repository tunnels. The space around each canister will be filled with pre-compacted bentonite which over time will draw in the surrounding ground water and swell, closing up any construction joints. However, for the purposes of performance assessment, it is necessary to consider the effect of glacial loading of a future repository and its impact on the mechanical behaviour of the bentonite, in particular, the sensitivity of total stress to changes in porewater pressure (backpressure).

Two experimental histories have been undertaken using a custom-designed constant volume and radial flow (CVRF) apparatus. In both tests backpressure was varied in a number of incremental and decremental cycles while total stress, porewater pressure and volumetric flow rate were continuously monitored.

The swelling pressure of the buffer clay at dry densities of 1.58 Mg m^{-3} and 1.61 Mg m^{-3} was determined to be around 5.5 MPa and 7.2 MPa respectively. For initial ascending porewater pressure histories the average proportionality factor α ranged from 0.86 and 0.92. Data exhibited a general trend of increasing α with increasing backpressure. In test Mx80-11 this was supported by analysis of the water inflow data which indicated a reduction in system compressibility.

Asymptotic values of porewater pressure within the clay are in good agreement with externally applied backpressure values. Inspection of data provides no evidence for the development of hydraulic thresholds within the clay, subject to the boundary conditions of this test geometry.

Analysis of the stress data demonstrates significant hysteresis between ascending and descending porewater pressure histories. The amount of hysteresis appears to be linked to the magnitude of the backpressure applied to the specimen, suggesting some form of "stress memory" may occur within the clay.

At porewater pressures of 46 MPa the bentonite retains between 48 and 67% of its original swelling pressure depending on the test cycle. The data indicates a reduction in the rate of decline in swelling pressure as backpressure increases, indicative of a rise in α values at high water pressures. Linear regression suggests $\alpha = 1$ at a porewater pressure of 64 MPa. At the end of test Mx80-11 the average effective stress was 14.4 MPa (an increase of 100%). This has important implications for repository performance assessment.

No evidence of classic liquefaction was found in this experimental study.

This report describes an experimental study performed under SKB Purchase Order 13426.

Contents

1   Introduction

In the KBS-3 concept, composite copper and steel canisters containing spent nuclear fuel will be placed in large diameter disposal boreholes drilled into the floor of the repository tunnels. The space around each canister will be filled with pre-compacted bentonite blocks. Over time, the bentonite blocks will draw in the surrounding groundwater and swell, closing any construction gaps to encapsulate the waste in a low permeability barrier.

From a performance assessment perspective, the effect of glacial loading of a future repository and the resulting change in local porewater pressure is an issue that must be addressed. For a clay-water system with the porewater in thermodynamic equilibrium with an external reservoir of pure water at pressure, p_w, the total stress acting on the clay, σ, can be expressed as

$$\sigma = \sigma_i + R - A + p_w \tag{1}$$

where σ_i is the "interparticle stress" and R and A are the repulsive and attractive stresses respectively /Lambe 1960/. In conventional soil mechanics theory the effective stress σ_{eff} /Terzaghi 1943, Terzaghi and Peck 1967/ is defined as the difference between the total stress and the measurable pore pressure. Since distilled (pure) water was used in this experiment we can write the relationship:

$$\sigma_{eff} = \sigma - p_w = \sigma_i + R - A \tag{2}$$

For dispersed and highly plastic saturated materials such as bentonite which exhibit no mineral to mineral contact the interparticle term σ_i reduces to zero /Lambe and Whitman 1969/, and the effective stress equation simplifies to:

$$\sigma_{eff} = R - A \tag{3}$$

where R–A is equivalent to the swelling pressure, Π, of the clay. Recent work by /Harrington and Horseman 2003/ examining the sensitivity of total stress to changes in the externally applied water pressure demonstrated the general validity of the effective stress law. However, to account for minor departures in ideality, /Harrington and Horseman/ introduced a proportionality constant α (equal to $d\sigma/dp_w$) leading to:

$$\sigma = \Pi + \alpha\, p_w \tag{4}$$

where the proportionality constant α and was found to be in the range from 0.74 to 0.86.

The observation that α may not be equal to 1 has led to the suggestion that as the externally applied porewater pressure increases, swelling pressure (in this case equivalent to the effective stress) may actually decline to the point where liquefaction of the bentonite occurs /SKB 2005/.

Figure 1-1 shows a plot of the /Harrington and Horseman/ data in the same coordinate space as that presented by /SKB 2005/, where the swelling pressure of the clay is equivalent to the effective stress. Linear extrapolation of the data in a similar manner to that of SKB gives an apparent intercept of zero effective stress at a porewater pressure of 38.7 MPa, close to the value estimated by SKB of 33.4 MPa. The inference being that at water pressures around 33 to 38 MPa, liquefaction of the bentonite buffer may theoretically occur.
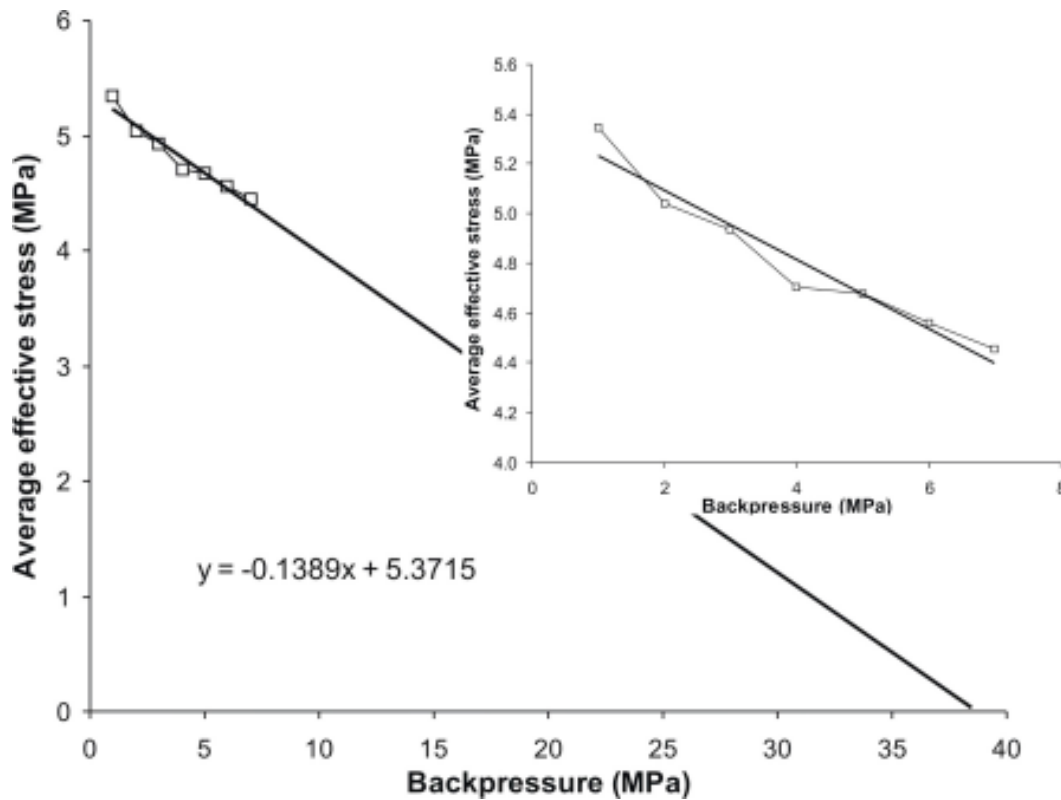
Figure 1-1. Extrapolation of swelling pressure data assuming continuous linear behaviour from /SKB 2005/. The insert graph (top right) shows the fit to the data in more detail. It is clear from the graphs that linear extrapolation of the data is inappropriate.

However, according to conventional theory, in order for liquefaction of bentonite to occur the clay platelets (which comprise the vast majority of the mineral constituents of the buffer) would have to move sufficiently far apart so that surface interactions cease to play a significant role in the shear strength of the material. Classically, this occurs when the water content of the clay increases to a point where shear strength reduces to a minimal value. In geotechnical terminology this point is known as the liquid limit. For Wyoming bentonite, /Donohew et al. 2000/ quote a value for this parameter of 332%. Given that the start moisture content of the KBS-3 material used in this study ranged from 25.6% to 26.7%, it is difficult to envisage under the constant volume conditions of the BGS apparatus, how the moisture content of the clay could sufficiently increase to the point where liquefaction occurs. Unless an alternative mechanism can be identified, it seems highly unlikely that liquefaction of the clay will occur.

This technical report presents the original results from /Harrington and Horseman 2003/, outlines some of the uncertainties associated with extrapolation of the data presented in Figure 1-1 and discusses in detail a new test history performed at elevated porewater pressures up to 46 MPa.

10

2   Experimental system

The constant volume and radial flow (CVRF) apparatus was originally designed to examine the sensitivity of gas flow in buffer bentonite to the test boundary conditions /Horseman et al. 2004/. Conceptually, the apparatus reproduces some of the main features of the repository near-field, including the borehole, the corroding canister and conductive fractures in the host rock.

There are six main components: (1) a thick-walled stainless steel pressure vessel, (2) a fluid injection system, (3) three independent backpressure systems, (4) five total stress sensors to measure radial and axial stress, (5) a porewater pressure sensor, and (6) a microcomputer-based data acquisition system.

The pressure vessel comprises a dual-closure tubular vessel manufactured from 316 stainless steel and pressure-tested at 69 MPa. Each of the end-closures is secured by twelve high tensile cap-screws which can also be used to apply a small pre-stress to the specimen if required. Figure 2-1 is a cut-away section showing the two end-closures with their embedded drainage filters and axial total stress sensors, the central fluid injection filter, the twelve radial sink filters, the three radial total stress sensors and the porewater pressure sensor.
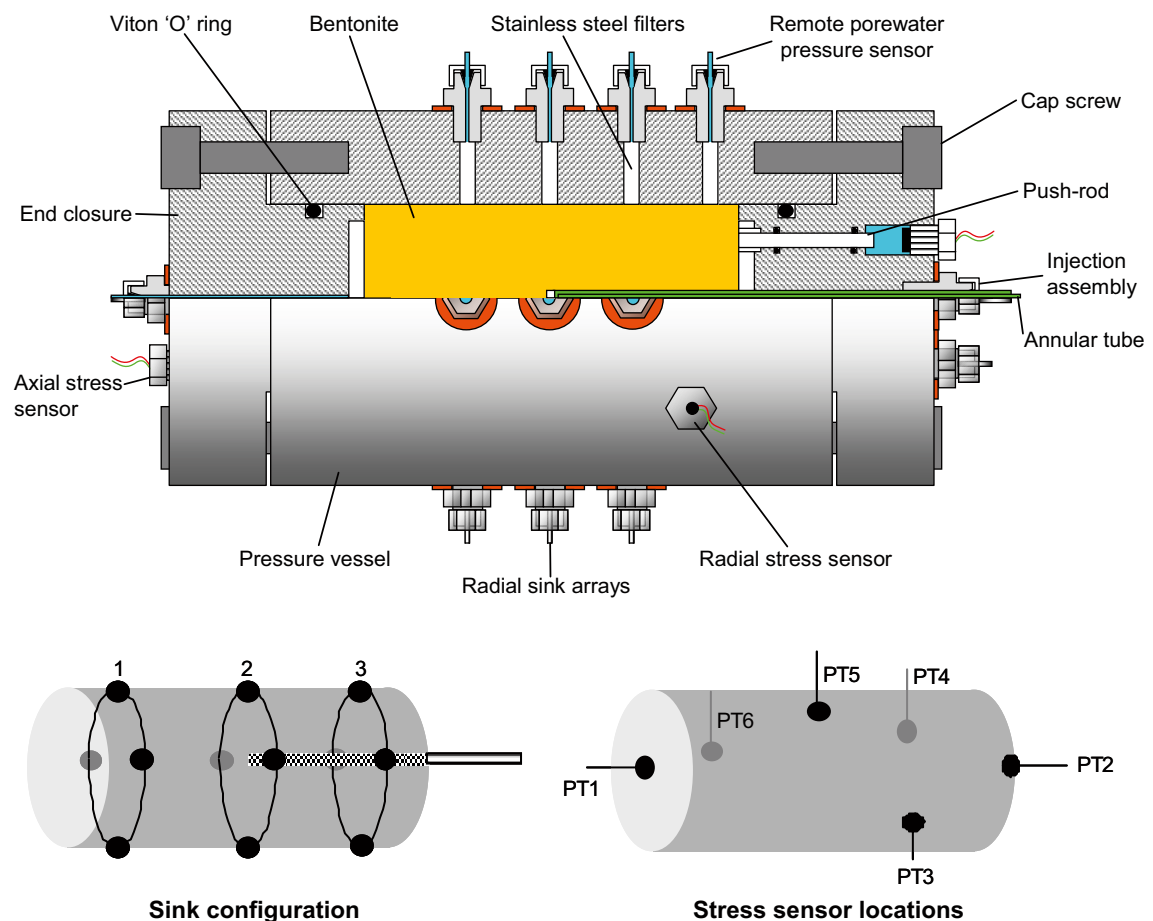

Figure 2-1. *Cut-away diagram of the constant volume and radial flow (CVRF) gas migration apparatus. Sensors are as follows: [PT1] – axial total stress on the backpressure end-closure, [PT2] – axial total stress on the injection end-closure, [PT3] – radial total stress close to the injection end-closure, [PT4] – porewater pressure close to the injection end-closure, [PT5] – radial total stress at the mid-plane, and [PT6] – radial total stress close to the backpressure end-closure.*

The 60 mm internal bore of the pressure vessel was honed to give a highly-polished surface. All ports, except those for the direct measurement of stress, contain sintered stainless steel porous plugs which are profiled to match the bore of the pressure vessel. The stress gauges are an in-house design which use a 6.4 mm steel push-rod fitted with an "O"-ring seal to compress a small volume of liquid contained within a chamber at the front face of a miniature Sensotec Model pressure transducer. In the porewater pressure sensor, the push-rod is replaced by a sintered stainless steel porous plug enabling water pressure to act on the front face of the transducer.

The central filter is embedded at the end of a 6.4 mm diameter stainless steel tube and is also used to inject the permeant, in this case distilled water. The end of the filter is profiled to match a standard twist drill.

Figure 2-2 shows a photograph of the injection end-cap, sintered stainless steel injection port, axial stress device and the large stainless steel drainage filter. Also visible is the small stainless steel push-rod which transmits the boundary stress, via a sealed reservoir filled with an incompressible fluid, to a miniature flat-face pressure transducer.

Pressure and flow rate of test fluid is controlled using an ISCO-100, Series D, syringe pump, operated by an ISCO pump controller. These units have an RS232 serial port, which allows volume, flow rate and pressure data from each pump to be transmitted to an equivalent port on a 32-bit personal computer. Additional test parameters are logged using an A/D converter card fitted to the computer. Typical acquisition rate is one scan per fifteen minutes.
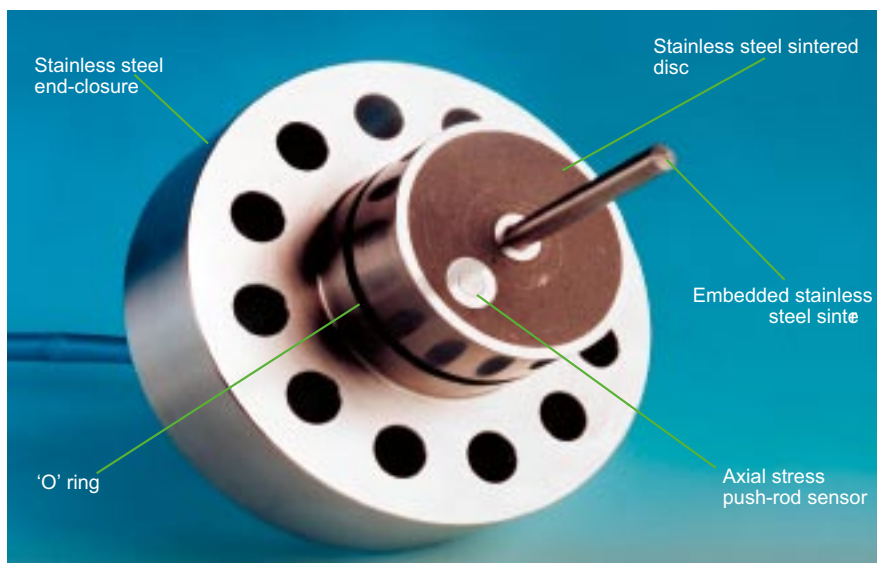

Figure 2-2. *Injection end-closure showing stainless steel sintered drainage disc, axial stress push-rod sensor, Viton 'O' ring and embedded injection filter.*

2.1   Calibration

All stress and pore pressure sensors were calibrated against laboratory standards by applying incremental steps in pressure, from atmospheric to a pre-determined maximum value. This was followed by a descending history to quantify any hysteresis. Least-squares fits were calculated and the regression parameters used to correct raw data. In test Mx80-11, raw pressure data are corrected by the application of a calibration curve of the form

$$p' = mp + c \qquad\qquad (5)$$

where p is the raw pressure reading, m and c are the calibration curve parameters, and p' is the corrected pressure. The calibration parameters m and c are not fixed but drift slowly with time, however it is not possible to determine them at every data point. Instead, they are obtained at a limited number of times, typically the beginning and end of the test, and it is assumed that they vary linearly with time through the test. Thus, m and c are given by

$$m(t) = m_1 + \frac{(m_2 - m_1)}{(t_2 - t_1)}(t - t_1) \qquad\qquad (6)$$

and

$$c(t) = c_1 + \frac{(c_2 - c_1)}{(t_2 - t_1)}(t - t_1) \qquad\qquad (7)$$

where m_1 and c_1 are the values of the calibration parameters at $t = t_1$, and m_2 and c_2 are the values at $t = t_2$. Thus to correct raw pressure data in the presence of a drifting calibration, the values of m and c are determined at each time point from equations (6) and (7), and these values are then used in equation (5) to obtain the corrected pressure.

Table 2-1 shows the changes of calibration parameters for each sensor in the test of sample Mx80-11. It can be seen that there is relatively little change in m, but a much larger change to c over the course of the experiment.

Table 2-1. Calibration parameters for test Mx80-11.

	Pump	AS1	AS2	RS1	RS2	RS3	PP1
m_1	0.9946	6943.0399	6976.6338	7052.6798	7590.8686	6961.4125	6875.5960
m_2	0.9946	6995.047	7106.056	7048.604	7606.557	6956.976	6850.602
c_1	37.7477	2850.9222	3088.0520	2300.4985	1886.1485	915.2315	2517.4923
c_2	22.569	3510.261	3644.366	2724.466	2514.941	1252.633	2591.455

2.2 Sample preparation

Pre-compacted bentonite blocks with a dry density of 1.58 and 1.60 Mg m^{-3} were manufactured by Clay Technology AB (Lund, Sweden) by rapidly compacting Mx-80 bentonite granules in a mould under a one-dimensionally applied. On receipt at BGS Keyworth, the preserved blocks were stored in a refrigerator prior to specimen preparation. Cylindrical test specimens with a diameter 60 mm and length 120 mm were manufactured by hand-trimming using a tubular former with a sharpened leading edge. The upper and lower surfaces were finished using a scraping action with a flat-bladed knife, leaving the end surfaces flat and parallel.

The former was mounted in a lathe and a 6.4 mm diameter hole drilled in the clay to accommodate the source filter and tubing assembly. The specimen was then extruded from the former into the pressure vessel using a screw-driven press. In test Mx80-11 two additional holes with diameters of 10 mm and 6.4 mm were drilled in the specimen while housed in its protective former. Machined lead weights profiled to match a standard twist drill were inserted into each hole prior to extrusion of the specimen into the apparatus. Figure 2-3 shows the initial layout and configuration of the lead weights relative to the central injection filter.

2.3 Physical properties

Table 2-2 shows the basic physical properties of each test specimen. Water content was determined by oven-drying at 105°C for a period in excess of 24 hours. Void ratio, porosity and degree of saturation are based on an average grain density for the bentonite of 2.77 Mg m^{-3}.

Table 2-2. Basic physical properties of the test specimens.

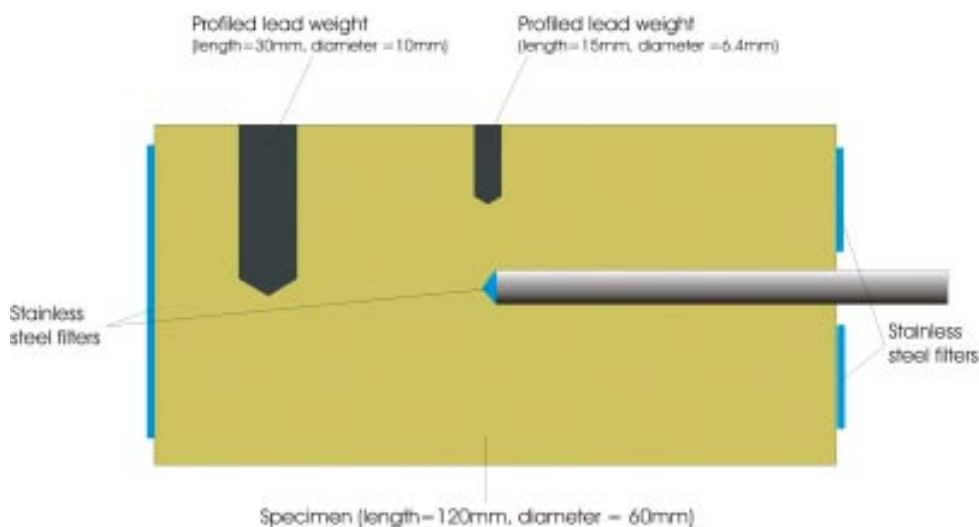| Specimen number	Block number	Water content (wt %)	Bulk density (Mg m^{-3})	Dry density (Mg m^{-3})	Void ratio	Initial saturation (%)
Mx80-10	BGS99	26.7	2.005	1.582	0.751	98.6
Mx80-11	–	25.6	2.016	1.605	0.726	97.6

Figure 2-3. *Cut-through of specimen Mx80-11 showing the location of the lead weights. Distilled water was also injected through all of the radial filters which are not shown in this diagram.*

3 Results

Section 3.1 contains a description of the original study performed by /Harrington and Horseman 2003/ on test specimen Mx80-10, which was subject to a maximum externally applied porewater pressure of 7.0 MPa. Section 3.2 contains a detailed description of a new test history specifically designed to examine the sensitivity of total stress at elevated externally applied water pressures up to a maximum value of 46 MPa.

3.1 Test Mx80-10

The specimen was exposed to de-aired and distilled water at a backpressure of 1.0 MPa which was applied to all filters. A swelling pressure of around 5.4 MPa was developed over 9 days of hydration. The sensitivity of total stress to moderate changes in the externally-applied water pressure was examined in this test history. Backpressure on the specimen was incremented in 1.0 MPa steps to a maximum value of 7.0 MPa, and then lowered to 4.0 MPa and finally to 1.0 MPa. The total stress and porewater pressure sensors were continually monitored (Figure 3-1). Data are presented in Table 3-1.

As the externally-applied water pressure increases, the total stress acting on the specimen becomes progressively more homogeneous. At the lowest backpressure value of 1.0 MPa, the variation in total stress across the specimen is around 0.6 MPa. At the highest backpressure value of 7.0 MPa, this difference decreases to under 0.1 MPa. Alpha values (a proportionality factor equal to $d\sigma/dp_w$) for each test stage are plotted in Figure 3-2. The data exhibits a general trend of increasing α with increasing backpressure. This behaviour may be linked to residual air bubbles moving into solution as the backpressure increases, or to changes in side-wall friction as total stress increases. The very slow rise in stress observed at the mid-plane radial stress sensor [PT5] also suggests that there may be a time lag in achieving full hydration in parts of the clay remote from the filters used for backpressuring. Examination of the data in Figure 3-1 clearly exhibits significant hysteresis between ascending and descending backpressure histories. A number of possible explanations for this behaviour were suggested by /Harrington and Horseman 2003/ and are discussed in Section 4.
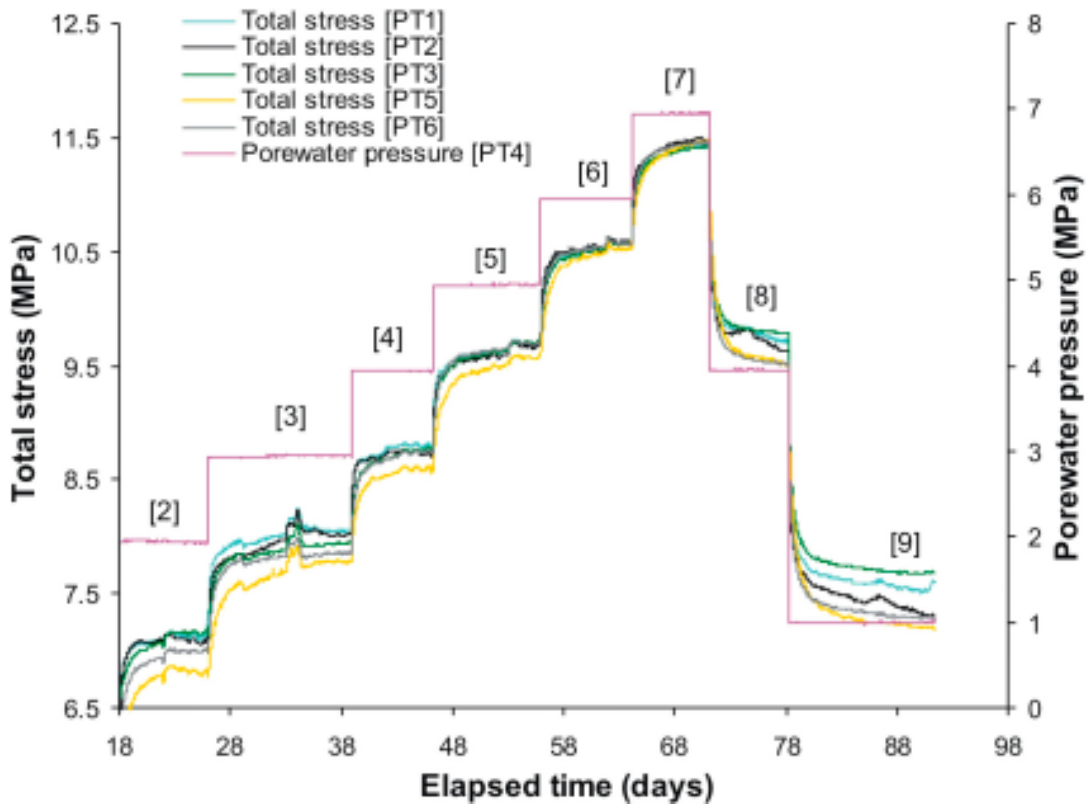
Figure 3-1. *Monitored changes in total stress on specimen Mx80-10 as external porewater pressure (backpressure) is incremented and decremented.*
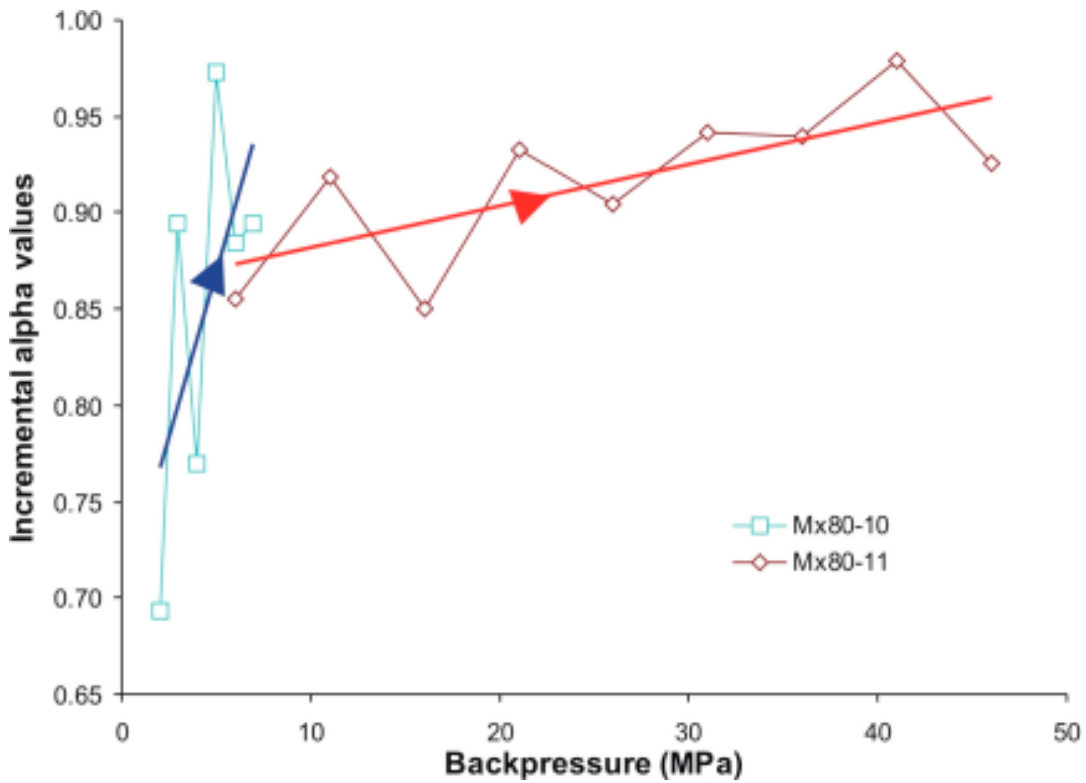

Figure 3-2. *Evolution of α for test stages [2] to [7] for Mx80-10 and [2] to [10] for Mx80-11. The solid blue and red lines represent least squares regression fits to the data. The difference in gradient between test histories may relate to differences in system compressibility.*

Table 3-1. Axial and radial total stresses in response to changes in applied backpressure. Values in parentheses represent porewater pressure measured on the periphery of the specimen by sensor PT4. Data for Mx80-10 taken from /Harrington and Horseman 2003/.

Test	Stage no.	Back-pressure (MPa)	Total stress (MPa)					
			Axial back-pressure end-cap [PT1]	Axial injection end-cap [PT2]	Radial injection end [PT3]	Radial middle [PT5]	Radial back-pressure end [PT6]	Average
Mx80-10	1	1.0	6.56	6.41	6.57	5.98	6.21	6.35
	2	2.0	7.27	7.07	7.12	6.76	6.97	7.04
	3	3.0	8.06	8.02	7.94	7.79	7.86	7.93
	4	4.0	8.77	8.70	8.75	8.57	8.73	8.70
	5	5.0	9.71	9.70	9.71	9.57	9.69	9.68
	6	6.0	10.56	10.58	10.56	10.53	10.57	10.56
	7	7.0	11.42	11.48	11.44	11.48	11.46	11.46
	8	4.0	9.72	9.64	9.78	9.50	9.51	9.63
	9	1.0	7.59	7.31	7.67	7.19	7.29	7.41
Mx80-11	1	1.0 [0.0]	8.46	7.42	7.93	8.42	8.69	8.19
	2	6.0 [6.0]	12.82	11.70	12.26	12.75	12.78	12.46
	3	11.0 [10.9]	17.37	16.31	16.92	17.43	17.24	17.05
	4	16.0 [15.9]	21.63	20.60	21.27	21.60	21.42	21.30
	5	21.0 [20.8]	26.32	25.22	25.92	26.32	26.05	25.97
	6	26.0 [25.8]	30.87	29.78	30.48	30.65	30.66	30.49
	7	31.0 [30.8]	35.65	34.64	35.44	34.70	35.54	35.20
	8	36.0 [35.8]	40.25	39.36	40.05	39.58	40.22	39.89
	9	41.0 [40.8]	45.18	44.52	45.26	43.75	45.22	44.78
	10	46.0 [45.7]	49.82	49.33	49.81	48.26	49.84	49.41
	11	31.0 [30.8]	39.19	38.55	38.74	37.76	39.21	38.69
	12	16.0 [15.8]	27.23	26.27	26.36	25.47	27.00	26.47
	13	46.0 [45.7]	50.69	50.94	50.46	48.80	51.27	50.43
	14	31.0 [30.7]	40.38	39.92	39.70	38.26	40.50	39.75
	15	46.0 [45.6]	50.90	50.92	50.40	49.12	51.01	50.47
	16	16.0 [15.9]	28.39	27.47	26.94	27.02	27.77	27.52
	17	1.0 [1.0]	16.77	15.15	14.55	14.99	15.26	15.34

3.2 Test Mx80-11

Test Mx80-11 was undertaken to examine the evolution of total stress at high externally-applied water pressures. As before the specimen was exposed to de-aired and distilled water at an initial backpressure of 1.0 MPa. A swelling pressure of around 7.2 MPa was developed over 6 days of hydration. While this value is higher than that of the previous test, it is more realistic of the candidate material currently under consideration by SKB in the KBS-3V disposal concept.

Backpressure on the specimen was increased in a stepwise manner in increments of 5.0 MPa, test stages [1] to [10], to a maximum value of 46 MPa. Backpressure was then varied in a number of decremental and incremental cycles, test stages [11] to [17], in order to examine the underlying hysteresis of the system and to provide an insight into the mechanisms and processes which may account for the non-ideality of the alpha parameter reported by /Harrington and Horseman 2003/. As before total stress and porewater pressure sensors were continuously monitored with time (Figures 3-3 and 3-4). Unlike the previous test the porewater pressure sensor [PT4] was isolated
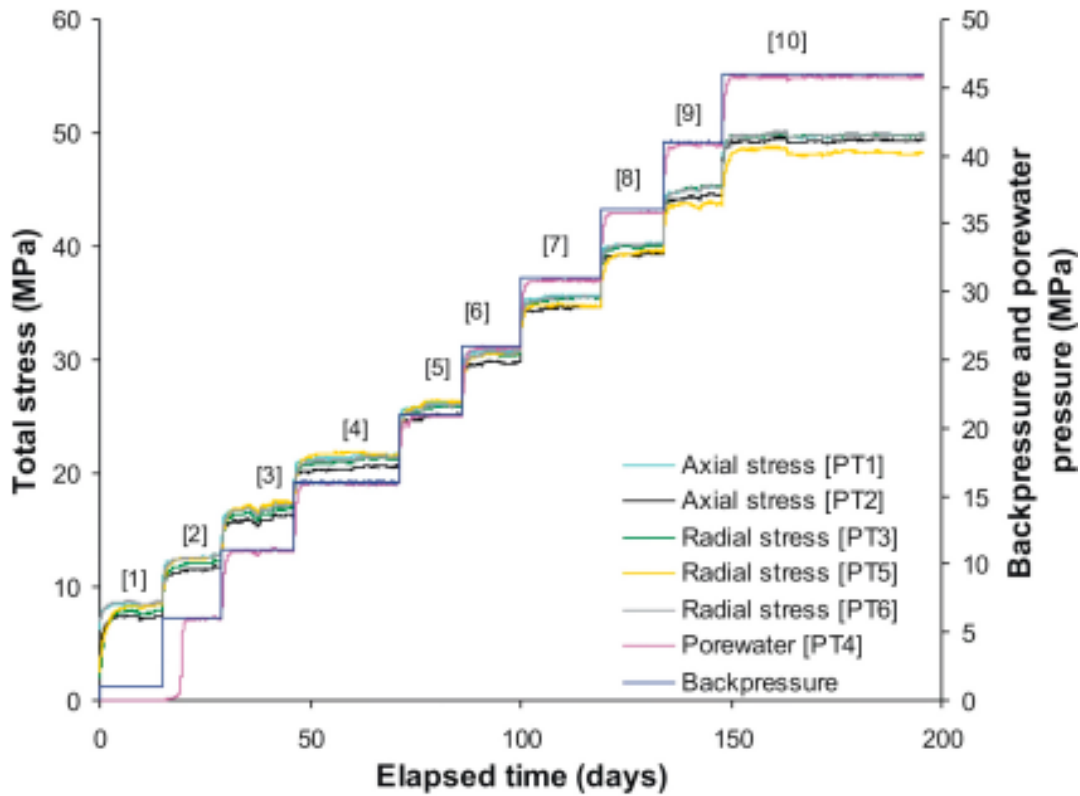
Figure 3-3. *Monitored changes in total stress for specimen Mx80-11, test stages [1] to [10] inclusive, for a history of increasing porewater pressure (backpressure).*
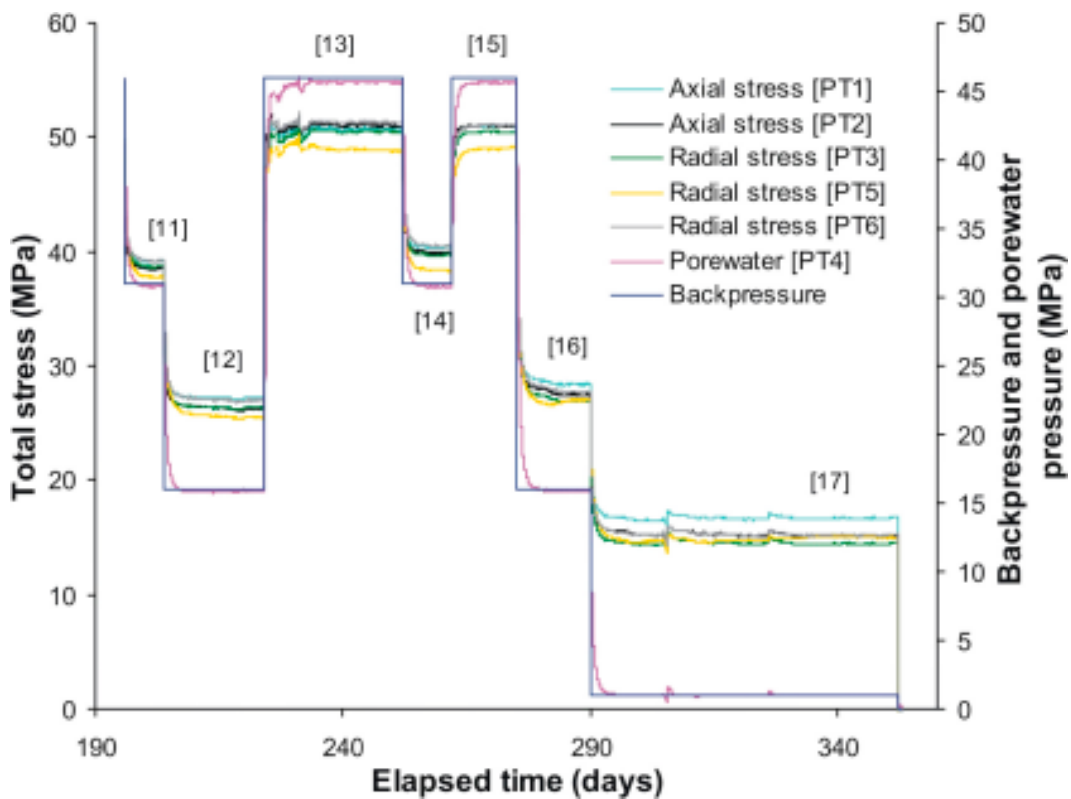

Figure 3-4. *Monitored changes in total stress for specimen Mx80-11, test stages [11] to [17] inclusive, as external porewater pressure (backpressure) is repeatedly decremented and incremented to examine hysteresis within the system.*

from the backpressure system in order to allow the evolution of porewater pressure on the surface of the specimen to be examined. Data from each test stage are presented in Table 3-1.

The rapid increase in porewater pressure observed by [PT4] at around 14.9 days corresponds to the increase in the externally applied backpressure from 1.0 to 6.0 MPa. The sudden rise in [PT4] pressure is accompanied by a sustained inflow of water from the backpressure system. This continued for around 1.7 days at which point the flux rapidly declined to a background level symptomatic of the slow progressive hydration of the clay. During this period around 9.0 ml of water was injected into the clay. Pre and post test measurements of specimen mass show only a small increase of 2.3 g occurred during the test history, comparable to the quantity of water required to saturate the clay. This clearly indicates that the vast majority of the observed inflow during test stage [2] was therefore into localised voids within the test system rather than the fabric of the clay.

Further examination of the data from sensor [PT4] indicates that the development of porewater pressure in the clay closely mirrors that of the total stress, exhibiting a time dependent response with each increment/decrement in backpressure, ranging from around 2 to 10 days in duration. Asymptotic values of porewater pressure taken from [PT4] for test stages [2] to [17] are in good agreement with the externally applied backpressure values. Analysis of the data demonstrates that within this test geometry, there is no evidence for the development of hydraulic thresholds within KBS-3 specification bentonite.

In contrast to test Mx80-10, the total stress data does not exhibit a systematic decrease in range (for a given backpressure) symptomatic of homogenisation of the stress field within the buffer as backpressure increases. From test stage [11] onwards, Figure 3-4, the backpressure applied to the specimen was varied to impose a number of decremental and incremental backpressure cycles. Analysis of the stress data during this time clearly demonstrates significant hysteresis exists when the externally applied backpressure is reduced. However, it is important to note that on re-pressurisation of the backpressure system, test stages [13] and [15], the asymptotic values of total stress are comparable with that obtained at the end of stage [10], suggesting the bentonite is behaving in a consistent and predictable manner.

As in the previous test, the average total stress measured during the initial ascending backpressure history exhibits a general trend of increasing α with increasing backpressure (Figure 3-2). The difference in gradient between the two test histories may reflect differences in system compressibility stemming from the high volumetric inflow observed at the beginning of stage [2].

The consistency in stress values measured along the different ascending/descending porewater pressure cycles for a given backpressure, cannot be explained through instrumentation hysteresis, compliance of the apparatus or instrumentation drift (the latter introducing minor errors as illustrated in Section 2.1). The systematic response of total stress to multiple cycles of ascending and descending backpressure suggest an underlying material property may be responsible for governing the behaviour of the system.

Figure 3-5 shows average α values and the resulting incremental inflows for test stages [2] to [10] plotted against applied backpressure. Linear regression of the data suggests α = 1 when backpressure increases to 64 MPa. However, this estimate should be treated with caution given the observed non-linearity in the effective stress behaviour (discussed in Section 4). As such, verification of this result requires experimental validation.

Analysis of water inflow data[1] measured for each test stage (plotted on the second y-axis of Figure 3-5) indicates a negative trend with increasing backpressure, symptomatic of a reduction in compressibility of the system. As discussed in Section 3-1 this behaviour may be explained by a number of factors including compression of residual gas, the movement of gas into solution and a reduction in general compliance of the apparatus at higher pressures.

A plot of net flow[2] into and out of the specimen for the entire test history (Figure 3-6) shows a similar response to that of total stress exhibiting significant hysteresis between ascending and descending backpressure histories. It is interesting to note that the hysteretic response is strongest for the second ascending backpressure history i.e. test stages [12] to [13], where the volume of water required to return the porewater pressure to 46 MPa is considerably less than that of the previous steps, indicative of a reduction in system compressibility. However, when backpressure was decreased for a second time, stage [14], a similar gradient to the initial descending history, i.e. stages [10] to [11], is observed. This general trend is repeated for subsequent backpressure histories of ascending and descending water pressure.

Analysis of the net inflow and geotechnical data indicates resaturation of the clay occurs early in the test history and is complete by the end of stage [2]. The subsequent inflow of water (Figure 3-6) must therefore be accommodated through expansion of the pressure vessel or compression, compaction and potential reorientation of the mineral fabric. While an elastic analysis of the pressure vessel subject to increasing internal stress has not been performed as part of this study, the non-linearity of the net inflow curve indicates compliance of the pressure vessel is not the primary cause of the observed hysteresis. It seems probable, given the non-linear behaviour in the inflow versus backpressure curve, that the water acts on and compresses the mineral fabric. It is conceivable that localised consolidation and or reorientation of the mineral assemblages could account for the irreversibility seen in the system. This hypothesis is discussed further in Section 4.

It is important to note that at the end of the test history when backpressure was reduced to the start value of 1.0 MPa, the average effective stress within the system was 14.4 MPa. This represents an increase in the total stress of 100% and would seem to suggest that the specimen exhibits some form of stress memorisation in response to a history of ascending and descending porewater pressure. If correct this has important implications for repository safety assessment.

Following decommissioning of the test, no movement of the profiled lead weights was observed.

---

[1] To mitigate pump and tube compliance, instantaneous changes in pump volume caused by a change in externally applied porewater pressure have been removed from the data by deleting the first logged cycle of each test stage.

[2] In the absence of representative data for stage [2] due to the large volumetric inflow observed at the beginning of this stage, net flow into the specimen is assumed to equal the average inflow observed during test stages [1] and [3].
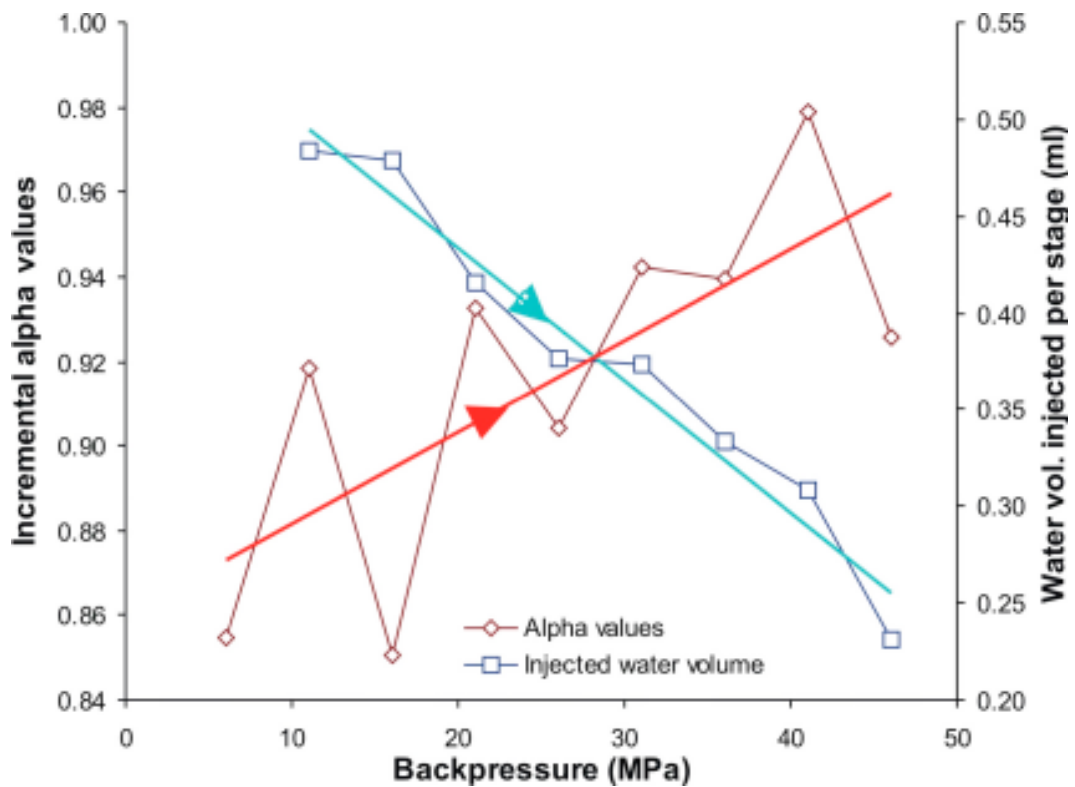
Figure 3-5. Alpha values for test stages [2] to [10] inclusive show a systematic rise in value as the applied backpressure increases. Conversely, the volume of water injected during each test stage exhibits a negative trend. This behaviour is symptomatic of a reduction in system compressibility. The solid blue and red lines represent least squares regression fits to the data.
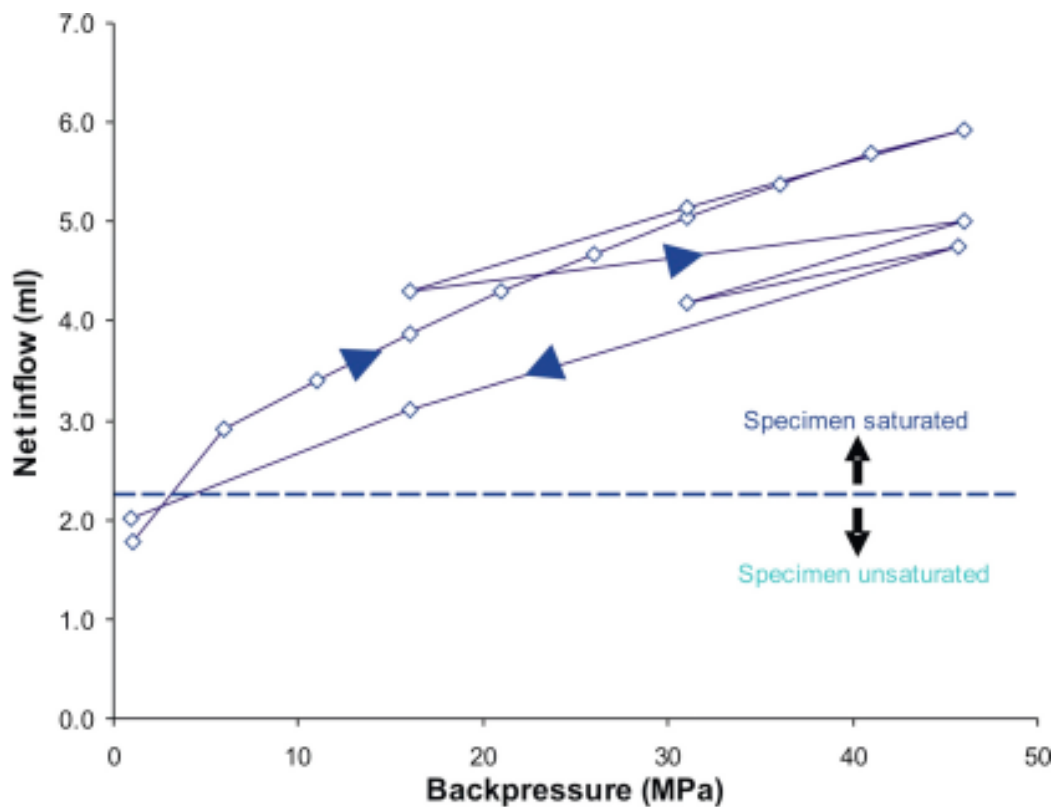

Figure 3-6. Corrected net inflow data for test history Mx80-11. Full saturation of the specimen is achieved early in the test history. A good mass balance is achieved across the entire test history.

4 Discussion

Figure 4-1 shows a plot of the average total stress against the applied backpressure for both test histories. Linear regression of the equilibrium stresses for the initial ascending history of porewater pressure gives $\alpha = 0.86$ and 0.92 for tests Mx80-10 and Mx80-11 respectively. Possible reasons for $\alpha \neq 1$ during this stage of testing include side-wall friction between the clay and the steel vessel, the presence of residual air bubbles in the clay and the finite compliance of the sensors used to measure the total stress. Extrapolation of the best-fit line to the intercept at zero backpressure for each test history gives $\Pi = 5.5$ MPa and 6.9 MPa respectively, both very close to the values obtained from the initial hydration stage of each test.

In extrapolation of the data presented in Figure 1-1 it is questionable to assume continuous linear behaviour to the x ordinate. If the departure from ideality in α was due to compression of residual gas, then this should exert a progressively smaller affect as porewater pressure increased. The data from test Mx80-10 shows the range in total stress responses actually reduce as water pressure rises and for the last stage ($p_w = 7$ MPa) converge to become almost identical. The α for this stage was ~0.9. This could be explained by a homogenisation in the compressibility of the clay as gas moves into solution. However, Mx80-11 does not exhibit the same characteristics even though the start saturations for both specimens were fairly similar. This may reflect differences in the system compressibility discussed earlier or relate to a change in resolution of the stress sensors which were replaced before the start of test Mx80-11.
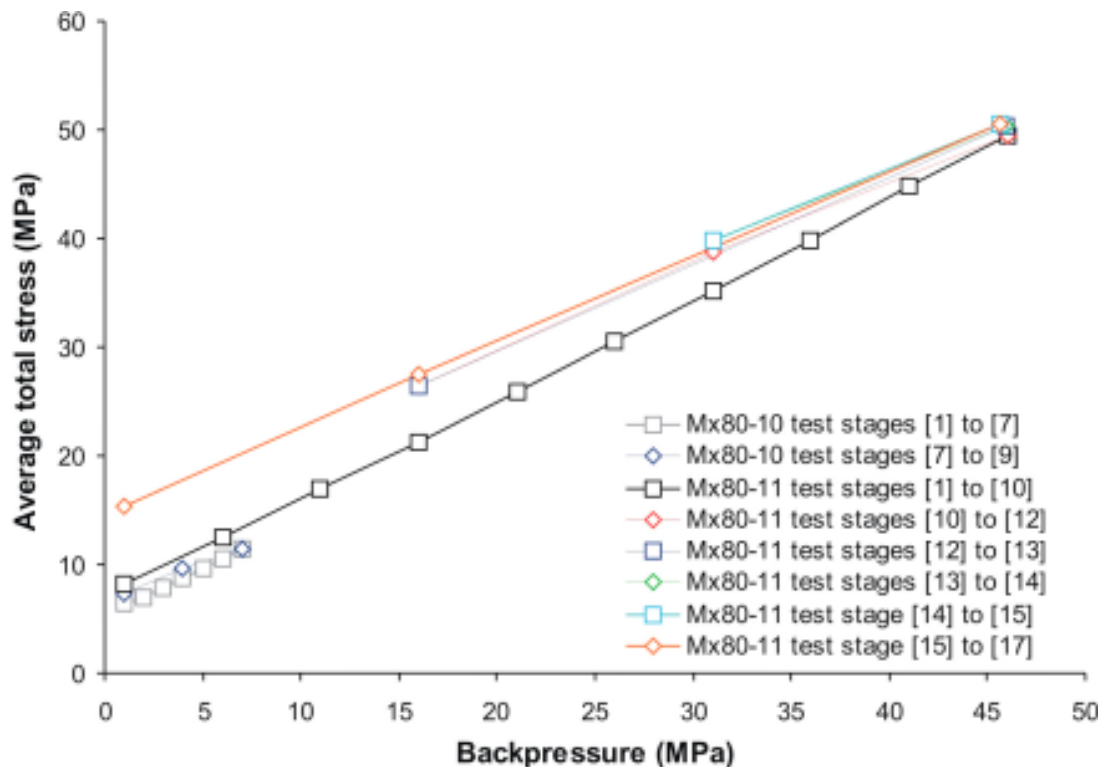

Figure 4-1. *Average total stress plotted against externally applied water pressure (backpressure). The data are presented in Table 3-1.*

23

Sidewall friction could also result in non-ideal behaviour and there is some evidence in the data from individual sensor values (Table 3-1) which show non-uniform increases in total stress between test stages, resulting in the possible introduction of a small frictional error. Additional reasons for $\alpha \neq 1$ may also include: interplatelet friction which is not included in the formulation of Equation [2]; compliance of the apparatus and measurement systems at high porewater pressures; compression of the mineral framework; changes in fabric/packing under high water pressures.

However, examination of the data (Figure 4-2) clearly indicates that at high porewater pressures Mx80 buffer clay retains a significant proportion of its swelling pressure and that the linear extrapolation of data presented in Figure 4-2 is wholly inappropriate. Indeed, at water pressures of 46 MPa the bentonite retains between 48 and 67% of its original swelling pressure depending on the test cycle. The first derivative of the data in Figure 4-2, for test stages [2] to [10] of Mx80-11, indicates a reduction in the rate of decline in swelling pressure as backpressure increases. This is indicative of a rise in α values at high water pressures. Linear regression of the derivative data suggests that the swelling pressure curve for Mx80-11 should reach an asymptote at a backpressure of around 64 MPa.

A cross-plot of effective stress versus backpressure for the entire data set presented in Table 3-1, shows a clear trend between the amount of hysteresis observed and the absolute magnitude of the backpressure applied to the specimen. The ratios x_1 to x_2 and y_1 to y_2 are both 0.15, suggesting that the observed hysteresis may in fact result from some kind of "stress memory", the strength of which is dependent on the magnitude of the backpressure applied to the specimen.

While the mechanism(s) governing this behaviour remain unclear, Figure 3-5 clearly indicates that the specimen continues to uptake water well beyond the point where fully saturated conditions would normally prevail, suggesting that the specimen in effect becomes "super saturated". Under such conditions it is possible that the aqueous phase acts on the mineral assemblages, resulting in some degree of localised change in both interparticle orientation and mineral spacing. When backpressure is reduced, the quasi-stable water composing the
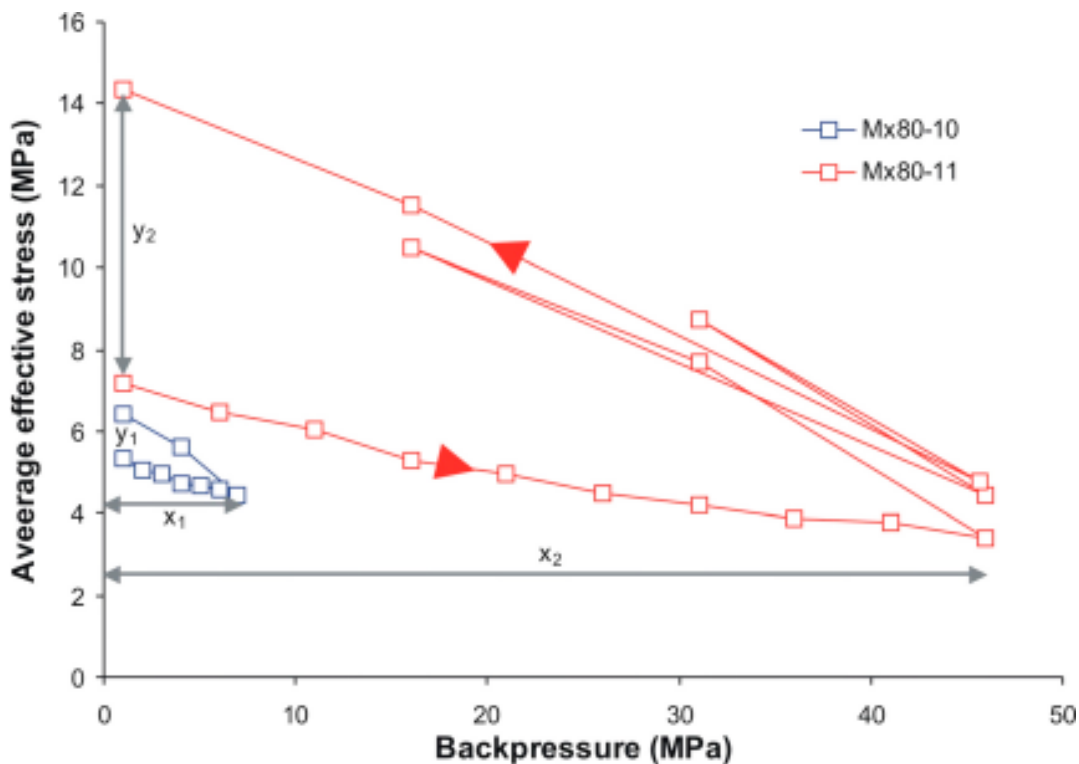

Figure 4-2. *Average effective stress plotted against backpressure for experimental histories Mx80-10 and Mx80-11. Inspection of the data clearly indicates that at high backpressures KBS-3 specification buffer bentonite retains a significant proportion of its effective stress (i.e. swelling pressure).*

super saturated fraction simply drains from the specimen (there is no data from this test to support the existence of hydraulic thresholds in KBS-3 buffer bentonite). The high residual stresses observed in the sample after testing may therefore be an artefact of irreversible strains associated with subtle changes in the fabric of the clay. While it is difficult to envisage mechanistically, fabric alteration could provide an explanation for both the apparent stress memory observed in the system and the small amount of water required during subsequent ascending backpressure cycles to achieve the same equilibrium conditions for a given back-pressure.

The tentative hypothesis presented above is purely speculative and further experimentation is required to improve process understanding in order to provide a sound basis for inclusion in performance assessment activities.

However, there is no evidence for liquefaction of the bentonite under the conditions imposed during this test programme.

5   Conclusions

The swelling pressure of the buffer clay at dry densities of 1.58 Mg m^{-3} and 1.61 Mg m^{-3} was determined to be around 5.5 MPa and 7.2 MPa respectively.

For conditions of varying externally-applied porewater pressure, p_w, the average total stress, σ, acting on the walls of the pressure vessel is given by the relationship

$$\sigma = \Pi + \alpha\, p_w \qquad\qquad\qquad\qquad (8)$$

where, Π, is the swelling pressure and α is a proportionality constant. Initial histories of ascending porewater pressure yield α values of 0.86 and 0.92 for tests Mx80-10 and Mx80-11 respectively.

During the initial ascending porewater pressure history both tests exhibit a general trend of increasing α with increasing backpressure. Analysis of the water inflow data for Mx80-11 indicates a similar trend, symptomatic of a reduction in system compressibility. The initial non-ideality of α can be explained by a number of factors such as interplatelet friction, compression of residual gas, the movement of gas into solution, sidewall friction and apparatus compliance. However, net inflow data indicates the specimen is fully saturated early in the test history, suggesting an alternative mechanism may exert a dominant role on the mechanical behaviour of the system.

Asymptotic values of porewater pressure measured on the surface of the specimen are in good agreement with the externally applied backpressure values. Changes in applied porewater pressure are generally mirrored within the specimen within around 2 to 10 days of the change in boundary condition. Inspection of data provides no evidence for the development of hydraulic thresholds within KBS-3 bentonite subject to these test conditions.

Analysis of the stress data clearly demonstrates significant hysteresis exists when externally applied backpressure is reduced. Comparison of effective stress data (i.e. swelling pressure) for both test histories indicates a clear trend between the amount of hysteresis observed and the absolute magnitude of the backpressure applied to specimen. Given the similarity in the x_1-x_2 and y_1-y_2 ratios it seems highly probable that the observed hysteresis results from some form of "stress memory" and not experimental compliance. The strength of this phenomena appears to be dependent on the magnitude of the backpressure applied to the specimen.

At porewater pressures of 46 MPa the bentonite still retains a significant proportion of its original swelling ranging between 48 and 67% depending on the test cycle. The data also indicates a reduction in the rate of decline in swelling pressure as backpressure increases, indicative of a rise in α values at high water pressures. Linear regression suggests $\alpha = 1$ at a porewater pressure of around 64 MPa.

At the end of test Mx80-11 the average effective stress was 14.4 MPa, represents an increase in the total stress of 100% and is an obvious artefact of the apparent stress memorisation mentioned above. If correct, this has important implications for repository performance assessment.

To improve process understanding further investigation is required to examine the evolution of the α parameter at higher water pressures and during the cyclic loading of porewater pressure. Additional studies should also focus on the cause of the hysteresis, its relationship to backpressure and any associated changes in material fabric.

No evidence of classic liquefaction was found in this experimental study.

6 References

Donohew A T, Horseman S T, Harrington J F, 2000. Gas entry into unconfined clay pastes between the liquid and plastic limits. Chapter 18. In: Environmental Mineralogy – Microbial Interactions, Anthropogenic Influences, Contaminated Land and Waste Management. Cotter-Howells J D, Campbell L S, Valsami-Jones E and Batchelder M. (eds), Mineralogical Society, London, Special Publication No. 9, 369–394.

Harrington J F, Horseman S T, 2003. Gas migration in KBS-3 buffer bentonite: Sensitivity of test parameters to experimental boundary conditions. SKB TR-03-02. Svensk Kärnbränslehantering AB.

Horseman S T, Harrington J F, Sellin P, 2004. Water and gas flow in Mx80 bentonite buffer clay. In: Symposium on the Scientific Basis for Nuclear Waste Management XXVII (Kalmar), Materials Research Society, Vol. 807. 715–720.

Lambe T W, 1960. A mechanistic picture of shear strength in clay. Proc. ASCE Res. Conf. Shear Strength of Cohesive Soils, 555–580.

Lambe T W, Whitman R V, 1969. Spoil mechanics. John Wiley, New York.

Terzaghi K, 1943. Theoretical soil mechanics. John Wiley, New York.

Terzaghi K, Peck R B, 1967. Soil mechanics in engineering practice. John Wiley, New York.

SKB, 2005. Personal communication by e-mail to author sent 31st Oct. 2005.

7   Acknowledgment